Crystal chemistry of brannockite, KLi₃Sn₂Si₁₂O₃₀, from a new occurrence in the Golden Horn Batholith, Washington State, USA

Markus B. Raschke[1,*], Evan J. D. Anderson[1], Julien Allaz[2], Henrik Friis[3], Joseph R. Smyth[2], Rudy Tschernich[4] and Randy Becker[5]

[1] Department of Physics, Department of Chemistry, and JILA, University of Colorado, Boulder, CO 80309, USA
*Corresponding author, e-mail: markus.raschke@colorado.edu
[2] Department of Geological Sciences, University of Colorado, Boulder, CO 80309, USA
[3] Natural History Museum, University of Oslo, Blindern, 0318 Oslo, Norway
[4] Moxee, WA 98936 USA
[5] Yakima, WA 98908 USA

Abstract: A second locality of the milarite-group mineral brannockite (ideally KLi₃Sn₂Si₁₂O₃₀) has been discovered at Liberty Bell/Washington Pass in the peralkaline granite of the Golden Horn Batholith, Okanogan County, Washington, USA as millimeter sized euhedral bladed clear crystals in a single miarolitic cavity. The Washington Pass brannockite shows micro-scale compositional zoning involving tetravalent A-site Sn^{4+}, Zr^{4+}, Ti^{4+}, and Hf^{4+} substitution and the coupled substitution $^A(X^{4+}) + {}^B\square \Leftrightarrow {}^A(Fe/Al)^{3+} + {}^B(Na,K)^+$. In contrast, brannockite analyzed from the type locality in the late hydrothermal zone of the Li-Sn-rich pegmatite of the Foote Mine, Kings Mountain, North Carolina, USA exhibits near end-member composition with only minor Na^+, Al^{3+}, and Ti^{4+}. Single-crystal X-ray diffraction of Washington Pass brannockite confirms the space group $P6/mcc$ with unit-cell parameters $a = 10.014(2)$ Å, $c = 14.268(5)$ Å, and $V = 1239.16(8)$ Å³. Washington Pass brannockite co-exists with its Zr-analogues, both the milarite-group sogdianite and the related tuhualite-group mineral zektzerite. Selected samples of both minerals show Sn as minor element. The sogdianite contains unusually low Na and Ti compared to most other localities and has near end-member composition. The results emphasize the high compatibility of the milarite structure with different heterovalent cations, associated with the cation-size dependent coupled distortion of the octahedral A and tetrahedral T2 sites.

Key-words: brannockite; Golden Horn batholith; Foote Mine; milarite group; tuhualite group; structure refinement; coupled substitution.

Introduction

The milarite-group minerals have the general formula $A_2B_2CD[(T2)_3(T1)_{12}O_{30}](H_2O)_x$ and space group $P6/mcc$. Many of the more than 25 species have only been discovered in the last few decades. The structure consists of $[Si_{12}O_{30}]$ six-membered double rings that are linked by tetrahedrally coordinated cations at the T2 site, and octahedrally coordinated cations at the A site. Stacking in the c-direction forms the C-site with 12-coordinated cations between the double rings (Forbes *et al.*, 1972; Černy *et al.*, 1980; Armbruster & Oberhänsli, 1988a; Hawthorne *et al.*, 1991).

The milarites exhibit large compositional variations at the T2 site with, *e.g.*, Li, Be, B, Mg, Al, Si, Mn, Fe^{2+}, Fe^{3+}, and Zn, and at the A-site with Al, Fe^{3+}, Sn^{4+}, Fe^{2+}, Mg, Zr, Ca, Na, Y, REE, Sc, and others (Sokolova *et al.*, 2000; Hawthorne, 2002). The associated large variations in cation radii can be accommodated by low-energy

distortions of edge-linked (T2)O₄ tetrahedra adjusting to predominantly regular AO₆ octahedra of variable size depending on the type of A-site cation. The resulting variations in site occupancy, coupled T2 and A-site polyhedral distortions, and end-member definition are of ongoing interest (Hawthorne, 2002; Geiger, 2009; Geiger & Grodzicki, 2012).

Table 1 shows the end-member composition and ideal site occupancies of the known Li-bearing milarite-group minerals. Brannockite, ideally $KSn_2Li_3Si_{12}O_{30}$, was described by White *et al.* (1973) from Li-Sn rich pegmatites of the Foote Mine, Kings Mountain, North Carolina, USA, and its structure refined by Armbruster & Oberhänsli (1988b). Closely related to brannockite, are the corresponding Zr end-member sogdianite $KLi_3Zr_2[Si_{12}O_{30}]$ (Dusmatov *et al.*, 1968; Boggs, 1984; Cooper *et al.*, 1999; Sokolova *et al.*, 2000) and the Ti end-member berezanskite $KLi_3Ti_2[Si_{12}O_{30}]$ (Pautov & Agakhonov, 1997). Coupled

Table 1. End-member composition and ideal site population for the Li-bearing milarite-group minerals.

	A	B	C	T2	T1
Brannockite[1]	$(Sn^{4+})_2$	$\square_2$	K	Li_3	Si_{12}
Sogdianite[2]	$(Zr^{4+})_2$	$\square_2$	K	Li_3	Si_{12}
Berezanskite[3]	$(Ti^{4+})_2$	$\square_2$	K	Li_3	Si_{12}
Sugilite[4]	$(Fe^{3+})_2$	Na_2	K	Li_3	Si_{12}
Darapiosite[5]	$(Mn^{2+})_2$	Na_2	K	Zn_2Li	Si_{12}

(1) White *et al*. (1973) and Armbruster & Oberhänsli (1988b).
(2) Dusmatov *et al*. (1968), Boggs (1984), Cooper *et al*. (1999), and Sokolova *et al*. (2000).
(3) Pautov *et al*. (1997).
(4) Armbruster & Oberhänsli (1988b).
(5) Semenov *et al*. (1975) and Ferraris *et al*. (1999).

substitution of Sn^{4+} in brannockite with trivalent cations and associated occupancy of the vacant B-site with Na^+ leads to sugilite $K(Na,\square)_2 (Fe^{3+},Mn^{3+},Al^{3+})_2 Li_3[Si_{12}O_{30}]$ (Armbruster & Oberhänsli, 1988b). Darapiosite $K(Na,K,\square)_2 (Mn^{2+}, Zr^{4+}, Y^{3+})_2 (Li, Zn, Fe^{2+})_3[Si_{12}O_{30}]$ (Semenov *et al*., 1975; Ferraris *et al*., 1999) in end-member composition with Zn_2Li in T2-site is charge balancing the divalent A-site with two Na^+ on the B-site (Hawthorne, 2002). Similar relationship applies to dusmatovite $K(\square, Na, K)_2 (Mn^{2+}, Zr^{4+}, Y^{3+})_2 (Zn, Li)_3[Si_{12}O_{30}]$ (Sokolova & Pautov, 1995; Pautov *et al*., 1996).

Here we investigate the crystal chemistry of brannockite, which we recently identified in the alkaline granite of the Golden Horn Batholith, near Liberty Bell/Washington Pass, Washington State, USA, as the first analysis of brannockite from outside the type locality. We provide a chemical and structural analysis and comparison of brannockite from the two different geological settings. In addition, we study the relationship of trace-element composition between brannockite, sogdianite and zektzerite from the Washington Pass locality. These results add to the understanding of the complex crystal-chemical and structural relationships within the milarite-group minerals.

Occurrence and geological setting

Brannockite has previously only been described from the type locality at the Foote Mine (White *et al*., 1973). The Foote Mine, located in the tin–spodumene belt of North and South Carolina, is one of several Li-bearing granite pegmatites (quartz–microcline–spodumene pegmatite) of Mississippian age (~340 Ma), intruded into the Cherryville quartz monzonite, schist, and amphibolite (*e.g.* White, 1981; Horton, 2008; Swanson, 2012). The pegmatite is generally unzoned and characterized by the absence of primary hydrous phases. It consists predominantly of primary microcline, quartz, and spodumene (~ 20 vol%) with accessory amounts of beryl, Mn-bearing fluorapatite, triphylite ($LiFePO_4$), and cassiterite.

In joints and under secondary hydrothermal influence, the mobilization of primary minerals gave rise to a solution enriched in Li, Be, K, Na, Mn, P, and Sn (Brown, 1982). Fluids crystallized in joints and fractures, and precipitated a complex assemblage of rare phosphate and silicate minerals, including several Li and Sn bearing minerals. In addition to brannockite, Sn-bearing minerals include Sn-rich titanite, wickmanite $MnSn(OH)_6$, and eakerite $Ca_2SnAl_2Si_6O_{18}(OH)_2 \cdot 2H_2O$ (Leavens *et al*., 1970; Kossiakoff & Leavens 1976). Eleven beryllium minerals have been identified including bertrandite $Be_4Si_2O_7(OH)_2$, bavenite $Ca_4Be_2Al_2Si_9O_{26}(OH)_2$, and milarite $(K,Na)Ca_2 Al[Be_2Si_{12}O_{30}] \cdot xH_2O$, as the only other milarite-group mineral.

The Golden Horn Batholith is a shallow peralkaline granitic intrusion of Eocene age (47–50 Ma) in the crystalline core of the North Cascades Mountains in Washington State (Misch, 1966; Stull, 1969; Boggs, 1984). There are chiefly four phases of granite intrusion in the batholith: a peralkaline arfvedsonite granite, a less alkaline transitional "border granite", and two different types of biotite granites (Boggs, 1984). The granites are unusually rich in otherwise rare, Zr-bearing silicate minerals. These include sogdianite $K(\square,Na)_2Li_3(Zr,Fe,Ti)_2 [Si_{12}O_{30}]$ (Dusmatov *et al*., 1968; Cooper *et al*., 1999; Pautov *et al*., 2000; Sokolova *et al*., 2000) and the related tuhualite-group mineral zektzerite $LiNa(Zr,Ti,Hf)[Si_6O_{15}]$ (Dunn *et al*., 1977; Boggs, 1984). Both minerals are in part rock forming, but also occur in miarolitic cavities as euhedral crystals up to several cm in size. In contrast to the Foote Mine, the Golden Horn Batholith is poor in beryllium minerals with only genthelvite $Zn_4Be_3(SiO_4)_3S$ and gadolinite group $(Y,REE)_2FeBe_2Si_2O_{10}$ minerals having been identified.

The Golden Horn brannockite described here was found in the early 1990's in a single miarolitic cavity (*ca*. 12 cm in diameter) in a talus boulder below Liberty Bell Mountain, close to Washington Pass. The host rock is an annite-bearing granite found within the transitional peralkaline "border granite" phase of the Golden Horn Batholith. The rock adjacent to the cavity has a graphic granite texture composed of white microcline, minor colorless quartz, and altered annite. Amphiboles are not present in the cavity or in the immediately surrounding rock. Within the cavity, brannockite occurs as aggregates up to 2 mm in diameter of hexagonal crystals (Fig. 1a) on microcline. The brannockite crystals are partially coated with an unidentified clay mineral and chlorite-group mineral. Associated with the brannockite in the cavity are gadolinite-(Y) and kainosite-(Y).

Physical properties

Under short-wave UV light the Golden Horn brannockite crystals fluoresce pale yellow, similar to zektzerite and sogdianite. The crystals exhibit a simple morphology, with a dominant basal pinacoid {0001} and prisms {10$\bar{1}$0} (Fig. 1a, inset).

The Foote Mine brannockite studied for comparison was selected from euhedral crystals, occurring on a matrix containing quartz, albite, and mica. In contrast to the brannockite found at Liberty Bell/Washington Pass, the Foote
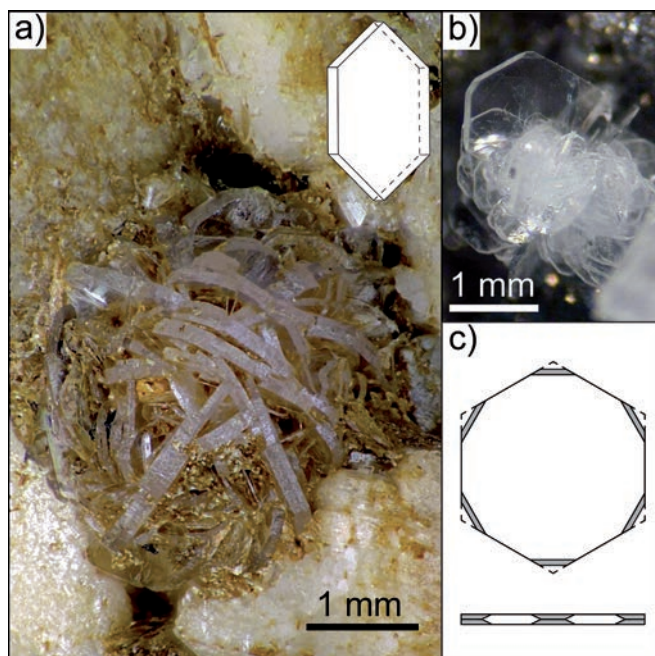
Fig. 1. (a) Brannockite cluster on microcline from Liberty Bell/Washington Pass, Golden Horn Batholith, Washington, USA, with schematic drawing of idealized hexagonal morphology (inset). Distinct crystal habit of brannockite from the type locality Foote Mine, Kings Mountain, North Carolina (b, photo courtesy Jason Smith), with idealized crystal drawing (c). (online version in colour)

Mine crystals fluoresce blue-white under short-wave UV light. The crystals occur as thin hexagonal plates (Fig. 1b), with a dominant basal pinacoid $\{0001\}$, small prisms $\{10\bar{1}0\}$ and $\{11\bar{2}0\}$ and a beveling dipyramid $\{11\bar{2}4\}$ (Fig. 1c).

Material and analytical methods

Three different individual brannockite crystal grains from the Washington Pass locality, labeled #1, #2, and #3, were selected, mounted in arbitrary orientation, and polished for electron microprobe (EMP) analysis. For comparison, one sogdianite and one zektzerite crystal from Washington Pass were prepared and analyzed under the same conditions. Nineteen quantitative analyses at different sample locations were obtained on crystal #1. Two brannockite crystals from the Foote Mine were analyzed, oriented parallel and perpendicular to the c-axis. A total of 30 analyses were obtained from the two Foote Mine samples. For X-ray diffraction and structure refinement, a fragment was taken from crystal #1 (#1) as well as one additional crystal #4 from the Washington Pass locality.

Polarized micro-Raman spectroscopy on polished sections and oriented crystals for both Foote Mine and Washington Pass brannockite reflect the characteristic optical phonon modes, the hexagonal crystal symmetry, and the absence of H_2O or bound OH groups (spectra in Fig. S1, freely available online as Supplementary Material linked to this article on the GSW website of the journal: http://eurjmin.geoscienceworld.org/).

Wavelength-dispersive compositional maps and quantitative microanalyses were obtained on a JEOL JXA-8600 electron microprobe (University of Colorado). Analytical conditions were 15 kV and 20 nA with a 5 μm beam diameter. Natural and synthetic standards were used (for details see Supplementary Material). The ZAF matrix correction from Armstrong (1988) was applied throughout. The Li-content was recalculated on a stoichiometric basis, assuming 3 Li and 30 O atoms per formula unit (apfu). All iron was assumed to be ferric as suggested by Mössbauer spectroscopy in the related milarite-group minerals sogdianite (Geiger & Grodzicki, 2012) and sugilite (Geiger, 2009).

For X-ray intensity measurement and unit-cell refinements a crystal fragment #1 from the grain mount of sample #1 was retrieved after completion of the microprobe analysis (Fig. 2a, dotted area) with approximate size $100 \times 150 \times 30$ μm³ (crystal #1). One additional single crystal of irregular shape measuring about $50 \times 50 \times 50$ μm³ (crystal #4), was selected for comparison.

Single-crystal X-ray diffraction data were acquired on a Bruker P4 four-circle diffractometer (University of Colorado) equipped with a point detector, an APEX II CCD detector, and a rotating Mo-anode generator operating at 50 kV and 250 mA. Unit-cell parameters were
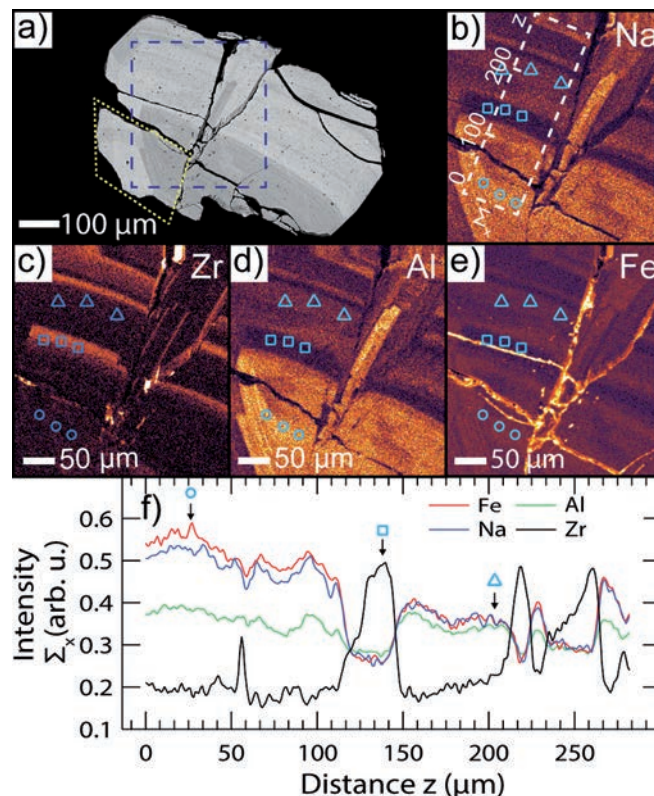

Fig. 2. Backscattered-electron image of Washington Pass brannockite crystal #1 (a). Elemental maps of area indicated in (a, blue dashed line) of Na (b), Zr (c), Al (d), and Fe (e). Corresponding line traces (f) along z-direction and signal averaged along the x-direction as indicated (dashed area in (b)). Symbols refer to analysis points in Table 2. Yellow dotted area in (a) indicates region of sample #1 retrieved for XRD analysis. (online version in colour)

refined from centering angles for 30 strong reflections with $10° < 2\theta < 30°$ each in both positive and negative 2θ regions using the point-detector. Data collection parameters are listed in Table 3. For the refinement of atom positions, anisotropic displacement parameters, and site occupancies, the program SHELXL-97 (Sheldrick, 2008) was used.

Results

Chemical composition

All three crystals from Liberty Bell/Washington Pass are compositionally zoned. Figure 2a shows a backscattered-electron image of crystal #1, exhibiting a core of lower average Z compared to the rim. Oscillatory zoning is observed throughout. A similar zonation is observed for crystals #2 and #3 (data not shown). Figure 2b-e shows compositional element maps (not background-corrected) for Na, Zr, Al, and Fe. Figure 2f shows a line trace of element variation for the area marked by the dashed inset in (b), averaged along the trend of constant concentration (Σ_x of counts in arbitrary units). There is a positive correlation of Fe and Na, and a negative correlation of Zr with Al, Fe and Na.

Table 2 gives the compositional range for crystal #1, with similar results for crystals #2 and #3. The composition of crystal fragment #1 used for XRD analysis is $K_{1.02(1)}Na_{0.10(8)}Li_3(Sn_{1.82(1)}Fe_{0.08(7)}Al_{0.05(2)}Zr_{0.04(5)}Ti_{0.009(3)}Hf_{0.005(2)})_{\Sigma 2.004}Si_{12}O_{30}$ based on an estimate of the modal abundance of the different zones.

The Foote Mine crystal shows only minor compositional variation (Table 2) and a composition close to end-member brannockite. Table 2 also shows averaged analyses of sogdianite and zektzerite crystals from Washington Pass. Sogdianite contains significant amount of Sn, Hf, Ti and minor amount of Na, Fe and Al. Zektzerite also contains significant Ti, Hf, Sn, Fe and Al.

Crystallography and structure refinement

The intensity data collection parameters and refined unit-cell parameters are given in Table 3. Selected bond distances derived from refinements using neutral-atom scattering factors are shown in Table 4 (for further details and atomic position coordinates and anisotropic displacement parameters, see Supplement, Table S1). The derived crystal structure is shown in Fig. 3 with its edge-linked distorted tetrahedral Li(T2) and regular octahedral Sn(A) sites, as well as the K(C), and vacant B sites.

Discussion

The large T2 tetrahedron (Li–O: 1.93 Å) shows strong angular distortion as a result of the small but regular A octahedron (Fig. 3). The associated strain is readily accommodated by the weak bonding of the LiO_4 tetrahedron, with an electrostatic bond strength of only 0.25 valence unit following Pauling's rule. This is in contrast to 0.67 valence unit for the edge-bonded A-site octahedron, thus preferring a regular shape (Geiger, 2009).

The tetra- and trivalent cations occupying the A-site of brannockite, *i.e.*, Sn^{4+}, Zr^{4+}, Ti^{4+}, Hf^{4+}, Fe^{3+} and Al^{3+}, sum to 1.96–2.04 (average 1.99(2)) for the Washington Pass, and 1.88–2.01 (average 1.95(3)) for the Foote Mine samples (Table 2). This suggests full occupancy of the A site. The close to ideal 12 Si apfu of the Washington Pass brannockite indicates exclusive occupancy of the T1 site with Si.

The total Na-content in Washington Pass brannockite stands out with a large spatial variation ranging from 0.03 to 0.20 apfu. The sum of alkalis ranges from 1.00 to 1.04 (average 1.02(1) apfu) for the Foote Mine analyses and 1.04–1.24 (average 1.13(6) apfu) for the Washington Pass sample. This suggests that the large C-site between the double-ring units is fully occupied by K and that excess alkali, especially Na, may occupy the B vacancy site, as discussed below.

Coupled cationic substitution

The ideal brannockite structure only contains mono- and tetravalent cations. To accommodate the trivalent cations Fe^{3+} and Al^{3+}, a coupled substitution is required. The variation of $(Al^{3+} + Fe^{3+})$ *vs.* $(Na^+ + K^+ - 1)$ for both Washington Pass and Foote Mine samples shows a linear correlation, with slope of 1.03(3) ($R^2 = 0.96$) and very
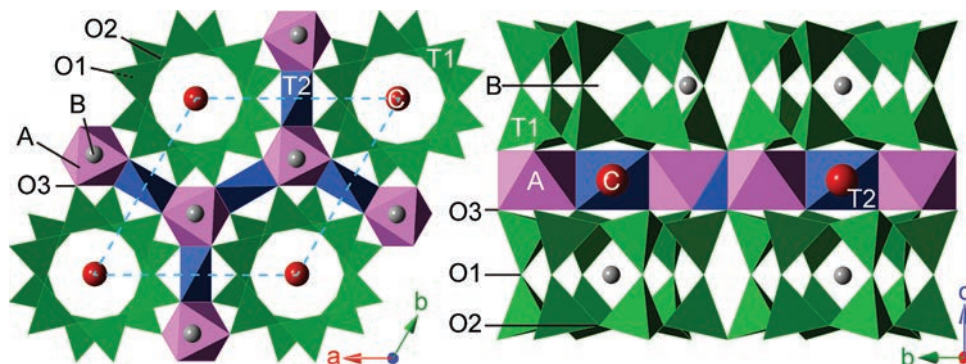

Fig. 3. Crystal structure of brannockite in two crystallographic orientations. (online version in colour)

Table 2. EMP analyses and formulae of compositionally zoned brannockite #1 from Washington Pass. Brannockite data from Foote Mine, as well as sogdianite and zektzerite data are included for comparison.

Wt.% oxide	Brannockite Golden Horn, Washington Pass							Foote Mine		Sogdianite Golden Horn		Zektzerite Golden Horn	
	Crystal Ideal	#1 Zr-poor Δ	#1 Zr-rich □	#1 Na/Fe-rich O	#1 Zr-absent	#1 Ti-richest	#1 Si-richest	Na-rich	Na-poor	Ideal	WP	Ideal	WP
Na_2O	–	0.22	0.09	0.50	0.25	0.06	0.23	0.07	0.01	–	0.14	5.85	6.09
K_2O	4.2	4.23	4.22	4.30	4.31	4.36	4.28	4.25	4.25	4.5	4.50	–	0.02
Fe_2O_3	–	0.38	0.14	1.16	0.65	0.12	0.68	<0.02	<0.02	–	0.14	–	0.37
Al_2O_3	–	0.25	0.08	0.28	0.31	0.05	0.24	0.11	0.17	–	0.08	–	0.28
ZrO_2	–	0.06	1.14	0.13	<0.03	1.18	0.21	<0.04	<0.04	23.3	19.7	23.27	18.9
SnO_2	27.1	25.2	24.4	23.6	24.6	24.5	24.4	25.9	25.9	–	1.66	–	0.47
TiO_2	–	0.09	0.07	0.04	0.03	0.11	0.08	0.03	0.08	–	0.23	–	0.94
HfO_2	–	0.06	0.12	0.07	0.08	0.12	0.10	<0.1	<0.1	–	0.67	–	0.58
MgO	–	–	–	–	–	–	–	0.01	0.01	–	–	–	–
Li_2O*	4.0	4.00	3.99	3.97	4.03	4.02	4.05	4.04	4.10	4.23	4.24	2.82	2.82
SiO_2	64.7	64.4	64.1	63.8	65.0	64.8	65.3	65.1	66.5	68.8	68.1	68.06	68.0
Total	100.0	98.8	98.4	97.9	99.3	99.3	99.6	99.5	101.0	100.0	99.43	100.0	98.45
apfu													
Na (B)	–	0.08	0.03	0.18	0.08	0.03	0.11	0.03	0.004	–	0.05	2	2.09
K (B)	–	0.01	0.01	0.03	0.02	0.03	0.01	–	–	–	0.01	–	0.003
$\sum^{(Na,K)}$ (B)	vac.	0.09	0.04	0.22	0.1	0.06	0.12	0.03	vac.	vac.	0.06	n.a.	n.a.
K (C)	1	1	1	1	1	1	1	1	0.99	1	1	n.a.	n.a.
Fe^{3+}	–	0.05	0.019	0.16	0.05	0.02	0.09	–	–	–	0.018	–	0.05
Al^{3+}	–	0.06	0.017	0.06	0.07	0.011	0.05	0.03	0.04	–	0.017	–	0.06
Zr^{4+}	–	0.006	0.10	0.012	–	0.11	0.02	–	–	2	1.69	2	1.62
Sn^{4+}	2	1.87	1.83	1.77	1.86	1.81	1.78	1.92	1.88	–	0.12	–	0.03
Ti^{4+}	–	0.012	0.010	0.006	0.007	0.016	0.01	0.002	0.012	–	0.03	–	0.13
Hf^{4+}	–	0.003	0.007	0.004	0.004	0.007	0.005	–	–	–	0.03	–	0.03
$\sum^{(3+,4+)}$ (A)	2 (Sn)	2.00	1.98	2.02	1.99	1.97	1.96	1.95	1.93	2 (Zr)	1.92	2	1.92
Mg	–	–	–	–	–	–	–	0.01	0.01	–	–	–	–
Li_{fixed} (T2)	3	3	3	3	3	3	3	3	3	3	3	2	2
Si (T1)	12	12.01	12.02	11.99	12.02	12.02	12.03	12.05	12.08	12	12.11	12	12
O_{fixed}	30	30	30	30	30	30	30	30	30	30	30	30	30
Total	18	18.1	18.0	18.2	18.11	18.05	18.11	18.0	18.0	18	18.1	18	18.0

Notes: symbols Δ, □, and O represent the averages of three analyses each for the zones indicated in Fig. 2(b-e).
* based on ideal stoichiometry.
n.a.: not applicable, vac.: vacancy.

Table 3. Crystal structure refinement data for brannockite from Washington Pass (#1 and #4) compared to data from Foote Mine (Armbruster & Oberhänsli, 1988b).

	#1	#4	Foote Mine[a]
a (Å)	10.014(2)[b]	10.001(6)[b]	10.002(2)
c (Å)	14.268(5)[b]	14.248(8)[b]	14.263(3)
V (Å³)	1239.162(6)	1233.7(2)	–
Space group	$P6/mcc$	$P6/mcc$	$P6/mcc$
Z	2	2	2
Radiation	Mo$K\alpha$	Mo$K\alpha$	Mo$K\alpha$
2θ range	0–64.11°	0–60°	0–80°
Reflections measured	11431	29808	–
Unique reflections	755	949	1127/117
$F_0 > 6\sigma F$	–	–	914/575
$R(\sigma)$	0.0247	0.0194	
R_{int}	0.0639	0.0702	–
R_w	–	–	0.042
R	0.0336[c]	0.0359[c]	0.042[d]

[a]Armbruster & Oberhänsli, 1988b.
[b]Unit-cell refinement obtained from point-detector data.
[c]Using neutral-atom scattering factors.
[d]Armbruster & Oberhänsli values for $F_0 > 6\sigma F$.

Table 4. Selected interatomic distances (Å) for brannockite from Washington Pass in comparison to data from Foote Mine.

	#1	#4	Foote Mine[a]
K site (C)			
K – O2 (12)	3.042(2)	3.037(2)	3.055(3)
Polyhedral volume ($Å^3$)	60.97	60.64	
Sn octahedron (A)			
Sn – O3(6)	2.022(2)	2.018(2)	2.014(3)
Polyhedral volume ($Å^3$)	11.30	11.24	
Quadratic elongation	1.0028	1.0029	
Li tetrahedron (T2)			
Li – O3(4)	1.931(2)	1.927(2)	1.927(4)
Polyhedral volume ($Å^3$)	3.23	3.21	
Si tetrahedron (T1)			
Si – O1(1)	1.607(1)	1.603(1)	1.602(1)
Si – O2(1)	1.619(2)	1.617(2)	1.620(4)
Si – O2(1)	1.626(2)	1.625(2)	1.620(4)
Si – O3(1)	1.591(2)	1.589(2)	1.594(2)
Si – O3 Avg	1.611	1.609	1.609
Polyhedral volume ($Å^3$)	2.088	2.079	
Quadratic elongation	1.0025	1.0025	

[a]Armbruster & Oberhänsli, 1988b.

small offset of 0.005 (Fig. 4a), suggesting the coupled substitution:

$$^A(X^{4+}) + {}^B\square \Leftrightarrow {}^A(Fe^{3+}, Al^{3+}) + {}^B(Na^+, K^+). \qquad (1)$$
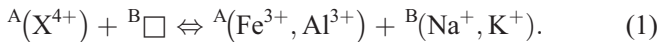
Correspondingly, $(Al^{3+} + Fe^{3+} + Na^+ + (K^+ - 1))$ *vs.* the sum of all tetravalent cations, $\sum A^{(4+)} - 12$, including Si^{4+}, are correlated with a slope of $-1.982(12)$ ($R^2 = 1.00$) and intercept at $2.00(17)$ (Fig. 4b). This inverse correlation is in excellent agreement with the ideal slope of -2 implied by eq. (1), and $X^{4+} = 14$ for the maximum occupancy of $T1(12) + A(2)$. It suggests that the coupled exchange reaction (1) fully captures the relevant trivalent and tetravalent cation substitution.

The sum of all $2+$, $3+$, and $4+$ cations, including the excess Si^{4+}, *vs.* Sn^{4+} shows an inverse correlation with slope of $-0.963(14)$ and intercept at $[Sn^{4+}] = 2.01(3)$ ($R^2 = 0.99$; Fig. 4c). Despite the small amounts of Mn or Mg, neglecting either the excess of Si or Mn + Mg results in a less-well defined correlation. This suggests complete occupancy of the A-site by all $2+$, $3+$ and $4+$ cations.

The presence of Fe^{2+} might involve a coupled-substitution $^A(Fe^{3+}) + {}^B\square \Leftrightarrow {}^A(Fe^{2+}) + {}^B(Na,K)$. However, this substitution would imply a deviation from the correlation between trivalent and monovalent cations (Fig. 4a). This suggests that such a substitution is unlikely in the studied brannockite and provides indirect support that Fe is primarily trivalent.

Site occupancies

The results of the site-scattering refinements for the XRD data for crystals #1 and #4 are shown in Table 5. The resulting A-site scattering electrons per formula unit (epfu) is in good agreement with the site population derived from EMP analysis and assignment of all $3+$ and $4+$ cations to that site. A small B occupancy would agree with the expectation from the coupled substitution and resulting stoichiometric correlations discussed above.

End-member relationships

Figure 5 compares the composition of brannockite from Washington Pass and Foote Mine, with the Washington Pass sogdianite sample, and the range of reported sogdianite analyses from Washington Pass (Boggs, 1984) and the alkaline Dara-i-Pioz massif in northern Tajikistan (Dusmatov *et al.*, 1968; Cooper *et al.*, 1999; Pautov *et al.*, 2000; Sokolova *et al.*, 2000). Interestingly, the Foote Mine brannockite analyzed here exhibits nearly end-member composition, in contrast to the type specimen from White *et al.* (1973) who reported the formula $K_{0.86}Na_{0.26}Li_{2.75}Sn_{2.02}Si_{12}O_{30}$ for Foote Mine
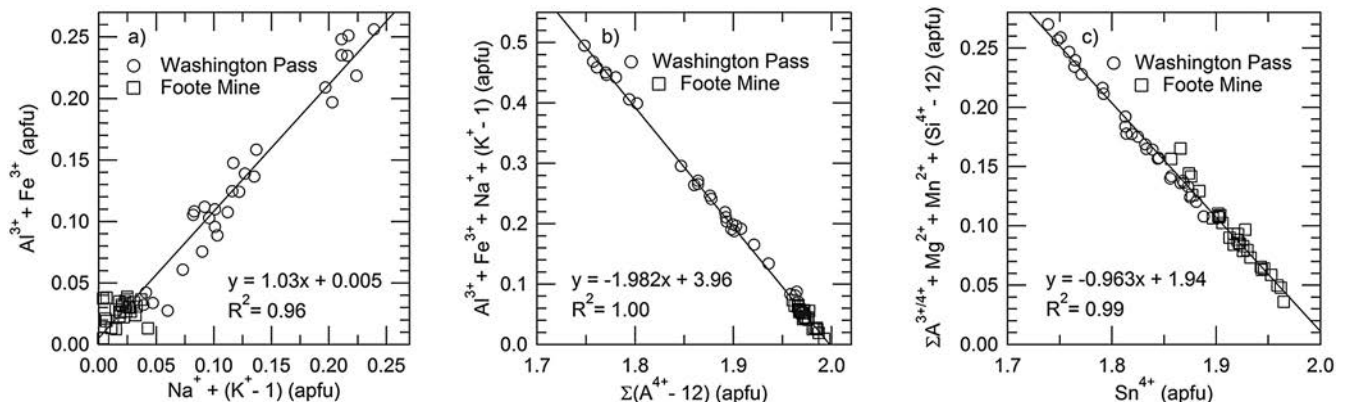

Fig. 4. Brannockite chemistry. (a) Positive correlation of $(Al^{3+} + Fe^{3+})$ *vs.* $(Na^+ + K^+ - 1)$. (b) Negative correlation of $(Al^{3+} + Fe^{3+} + Na^+ + K^+ - 1)$ *vs.* $\sum (A^{4+} - 12)$ including Si^{4+}. (c) Negative correlation of $(\sum A^{3+/4+} + Mg^{2+} + Mn^{2+} + Si^{4+} - 12)$ *vs.* Sn^{4+}. (online version in colour)

Table 5. Site-scattering refinement with site scattering (epfu) and site population assignment for crystal #1, compared to the results of EMP analysis.

Crystal	Site	Site scattering (epfu)	Site population (apfu)	Site population (from EMP average $\Delta+\square+O$)	Predicted site scattering from EMP (epfu)
#1	A	87.9(4)	1.91(1) Sn^{4+}	0.08(7) Fe^{3+} + 0.05(2) Al^{3+} + 0.04(5) Zr^{4+} + 1.82(1) Sn^{4+} + 0.009(3) Ti^{4+} + 0.005(2) Hf^{4+}	88.0(5)
	B	0.3(2)	0.03(2) Na^+	0.10(8) Na^+	1.0(8)
	C	17.6(2)	0.98(1) K^+	1.02(1) K^+	18.4(2)
	T2	6.1(3)	3.05(14) Li^+, or: 2.99(14) Li^++0.01(2) Na^+	3.00 Li^+ (fixed)	6
#4	A	87.9(3)	1.91(1) Sn^{4+}		
	B	0.3(2)	0.05(4)		
	C	17.1(2)	0.95(1) K^+		
	D	5.9(3)	2.95(13) Li^+		
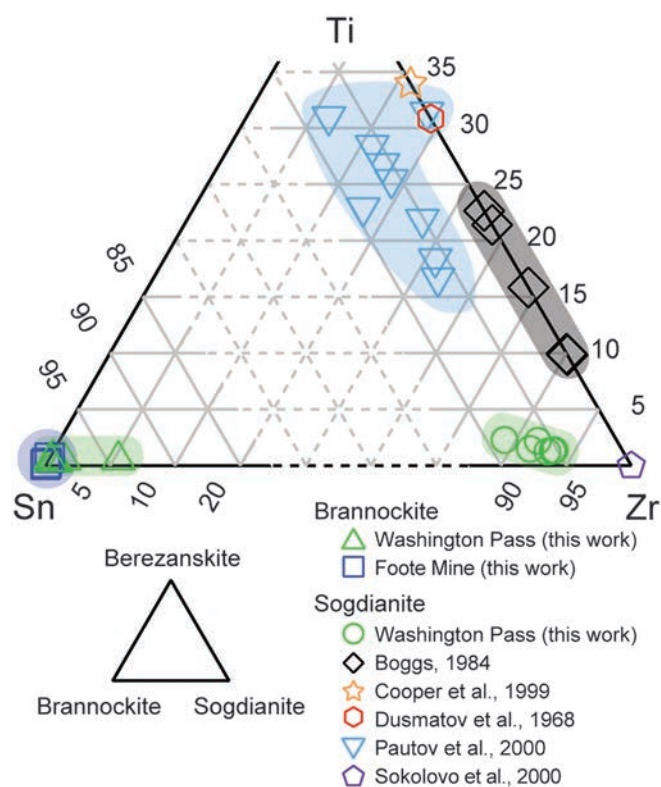
Fig. 5. Ternary diagram comparing data from this study and literature in the brannockite (Sn), sogdianite (Zr), and berezanskite (Ti) compositional field.

brannockite, on the basis of electron-microprobe and flame-photometry analysis.

Our analyzed sogdianite represents the first reported sogdianite containing Sn from Washington Pass, and is low in Ti. This is in contrast to earlier sogdianite analyses (Boggs, 1984), although it is unknown whether Boggs (1984) analyzed for Sn. The analyzed zektzerite also contains appreciable Sn, in contrast to earlier results (Dunn *et al.*, 1977; Boggs, 1984).

The substitution of Sn^{4+} in brannockite by trivalent cations and the corresponding occupancy of the B-site by Na^+ should lead to sugilite: $K(Na,\square)_2 (Fe^{3+},Mn^{3+},Al^{3+})_2 Li_3[Si_{12}O_{30}]$ (Armbruster & Oberhänsli, 1988b) (Table 1).

The EMP analyses of the three brannockite samples from Washington Pass show that they all have a core enriched in Zr and depleted in Na + Fe compared to the rim, indicating a change in the composition or temperature of the fluid crystallizing brannockite. Alternatively, the formation of another mineral in the cavity at this point could be responsible for this compositional change. Zircon, which is a common secondary phase in the cavities in Washington Pass, would preferentially partition all available zirconium in its structure, depleting the Zr-content in the co-existing brannockite.

At the Foote Mine pegmatites both Li and Sn are readily available with the presence of spodumene and cassiterite, respectively. In contrast, at Washington Pass there are no obvious Sn-minerals. Yet the Sn in at least some sogdianite and zektzerite suggests its wider presence than previously assumed. Both zektzerite and sogdianite occur as primary phases, and both commonly exhibit corroded crystal faces. This suggests that the alteration of these minerals can be a source for both Li and Sn for forming brannockite.

Structural relationships within the milarite group

The $<A–O>$ and $<T2–O>$ bond distances were found to scale linearly with the ion radii $<r_A>$ and $<r_{T2}>$, respectively (Hawthorne *et al.*, 1991; Ferraris *et al.*, 1999; Sokolova *et al.*, 2000; for details see Supplementary Material). For brannockite, a slight deviation from the linear correlation was found based on structure data of Armbruster & Oberhänsli (1988b) for Foote Mine brannockite, which we identify as likely corresponding to end-member composition. Hawthorne *et al.* (1991) suggested the unoccupied B site to be responsible for this deviation. Sugilite, with Li in T2 and B-site partially occupied by Na, does not deviate from the linear relationship (Armbruster & Oberhänsli, 1988b). A reduced deviation is observed for Washington Pass brannockite #1, with #4 in even perfect agreement with the relationship above, which correlates with the trend of a small but increasing B-site occupation

from #1 to #4. Alternatively, however, the possible presence of some minor amount of Al^{3+} on T2 could result in a smaller average radius bringing the $<T2–O>$ distance closer to the main trend.

The large compositional variability of milarite-group minerals is a result of the several crystallographic sites covering a wide range of size and coordination number. Therefore, small (*e.g.*, Be, B), large (*e.g.*, K, Na), monovalent (*e.g.*, Na, Li), or tetravalent (*e.g.*, Si, Sn) cations can be accommodated. This accommodation involves lattice distortion that can be correlated with site occupancy, ion radius and bond-strength ratio, especially on the A, B and T2 sites.

The analysis of structural correlations within the milarite group has long been of interest (*e.g.*, Forbes *et al.*, 1972; Černy *et al.*, 1980; Armbruster & Oberhänsli, 1988b; Hawthorne *et al.*, 1991; Ferraris *et al.*, 1999; Sokolova *et al.*, 2000; Lengauer *et al.*, 2009; Bojar *et al.*, 2011). The detailed chemical and structural analysis of brannockite as one additional member may help to address the overarching question on the origin of the unusually large chemical variability of the milarite structure type compared to other mineral groups.

In summary, the present study with the identification of multivalent substitutions in brannockite confirms end-member relationships of related milarite-group minerals. It reinforces previous conclusions regarding the role of B-site occupancy in the reduction of distortion on the A-site related to lower bond-strength ratio A/T2, similar to the conclusion drawn for sugilite (Armbruster & Oberhänsli, 1988b).

References

Armbruster, T. & Oberhänsli, R. (1988a): Crystal chemistry of double-ring silicates: Structural, chemical, and optical variation in osumilites. *Am. Mineral.*, **73**, 585–594.

Armbruster, T. & Oberhänsli, R. (1988b): Crystal chemistry of double-ring silicates: Structures of sugilite and brannockite. *Am. Mineral.*, **73**, 595–600.

Armstrong, J.T. (1988): Quantitative analysis of silicate and oxide materials: comparison of Monte Carlo, ZAF and $\varphi(\rho z)$ procedures. *in* ''Microbeam Analysis'', D. E. Newbury, ed. San Francisco Press Inc, San Fransisco, 239–246.

Boggs, R. (1984): Mineralogy and geochemistry of the Golden Horn Batholith, North Cascades, Washington. Ph.D. dissertation, University of California, Santa Barbara.

Bojar, H.P., Walter, F., Hauzenberger, C., Postl, W. (2011): Klöchite, $K\square_2(Fe^{2+}Fe^{3+})Zn_3Si_{12}O_{30}$, a new milarite-type mineral species from the Klöch volcano, Styria, Austria. *Can. Mineral.*, **49**, 1115–1124.

Brown, G.E, Jr. (1982): The mineralogy of pegmatites. *Am. Mineral.*, **67**, 180–189.

Černý, P., Hawthorne, F.C., Jarosewich, E. (1980): Crystal chemistry of milarite. *Can. Mineral.*, **18**, 41–57.

Cooper, M.A., Hawthorne, F.C., Grew, E.S. (1999): The crystal chemistry of sogdianite, a milarite-group mineral. *Am. Mineral.*, **84**, 764–768.

Dunn, P.J., Rouse, R.C., Cannon, B., Nelen, J.A. (1977): Zektzerite: a new lithium sodium zirconium silicate related to tuhualite and the osumilite group. *Am. Mineral.*, **62**, 416–420.

Dusmatov, V.D., Efimova, A.F., Kataeva, Z.T., Khoroshilova, L.A., Yanulov, K.P. (1968): Sogdianite, a new mineral. *Dokl. Akad. Nauk SSSR*, **182**, 1176–1177, (in Russian).

Ferraris, G., Prencipe, M., Pautov, L., Sokolova, E. (1999): The crystal structure of darapiosite and a comparison with Li- and Zn-bearing minerals of the milarite group. *Can. Mineral.*, **37**, 769–774.

Forbes, W.C., Baur, W.H., Khan, A.A. (1972): Crystal chemistry of milarite-type minerals. *Am. Mineral.*, **57**, 463–472.

Geiger, C.A. (2009): A ^{57}Fe Mössbauer spectroscopic study of sugilite, $KNa_2(Fe^{3+},Mn^{3+},Al)_2Li_3Si_{12}O_{30}$. *Can. Mineral.*, **47**, 927–931.

Geiger, C.A. & Grodzicki, M. (2012): A ^{57}Fe Mössbauer spectroscopic study of sogdianite: an example of a symmetric electric field gradient around Fe^{3+}. *Phys. Chem. Minerals*, **39**, 73–77.

Hawthorne, F.C. (2002): The use of end-member charge-arrangements in defining new mineral species and heterovalent substitutions in complex minerals. *Can. Mineral.*, **40**, 699–710.

Hawthorne, F.C., Kimata, M., Černý, P., Ball, N., Rossman, G.R., Grice, J.D. (1991): The crystal chemistry of the milarite-group minerals. *Am. Mineral.*, **76**, 1836–1856.

Horton, J.W. (2008): Geologic map of the Kings Mountain and Grover quadrangles, Cleveland and Gaston Counties, North Carolina, and Cherokee and York Counties. USGS Scientific Investigations Map, South Carolina, 2981 p.

Kossiakoff, A.A. & Leavens, P.B. (1976): The crystal structure of eakerite, a calcium-tin silicate. *Am. Mineral.*, **61**, 956–962.

Leavens, P.B., White, J.S, Jr, Hey, M.H. (1970): Eakerite - a new tin silicate. *Mineral. Rec.*, **1**, 92–96.

Lengauer, C.L., Hrauda, N., Kolitsch, U., Krickl, R., Tillmanns, E. (2009): Friedrichbeckeite, $K(\square_{0.5}Na_{0.5})_2(Mg_{0.8}Mn_{0.1}Fe_{0.1})_2(Be_{0.6}Mg_{0.4})_3Si_{12}O_{30}$, a new milarite-type mineral from the Bellerberg volcano, Eifel area, Germany. *Mineral. Petrol.*, **96**, 221–232.

Misch, P. (1966): Tectonic evolution of the Northern Cascades of Washington State. in ''Symposium on the Tectonic History, Mineral Deposits of the Western Cordillera in British Columbia and Neighbouring Parts of the United States; Special Volume, 8'', H. C. Gunning, ed. Canadian Institute of Mining and Metallurgy, Vancouver, B.C., 101–148.

Pautov, L.A. & Agakhonov, A.A. (1997): Berezanskite, $KLi_3Ti_2Si_{12}O_{30}$ a new mineral. *Proc. Russian Mineralogical Soc.*, **126**(**4**), 75–80, (in Russian).

Pautov, L.A., Agakhanov, A.A., Sokolova, E.V., Ignatenko, K.I. (1996): Dusmatovite, a new mineral of the milarite group. *Vestnik Mosk. Univ., Ser. 4 Geol.*, **N2**, 89–60, (in Russian).

Pautov, L.A., Khvorv, V.A., Agakhanov, A.A. (2000): Sogdianite and sugilite from the Dara-i-Pioz massif (Tajikistan). *Proc. Russian Mineralogical Soc.*, **129**, 66–79, (in Russian).

Semenov, E.I., Dusmatov, V.D., Khomayakov, A.P., Voronkov, A.A., Kazakova, M.Y. (1975): Darapiosite, a new mineral of the milarite group. *Zap. Vses. Mineral. Obshchest.*, **104**, 583–585, (in Russian).

Sheldrick, G.M. (2008): A short history of SHELX. *Acta Crystallogr.*, **A 64**, 112–122.

Sokolova, E.V. & Pautov, L.A. (1995): Crystal structure of dusmatovite. *Dokl. Phys.*, **40**, 607–610.

Sokolova, E.V., Hawthorne, F.C., Pautov, L.A. (2000): The crystal chemistry of Li-bearing minerals with the milarite-type structure: the crystal structure of end-member sogdianite. *Can. Mineral.*, **38**, 853–859.

Stull, R. (1969): The geochemistry of the southeastern portion of the Golden Horn Batholith, Northern Cascades, Washington. Ph.D. dissertation, University of Washington.

Swanson, S.E. (2012): Mineralogy of spodumene pegmatites and related rocks in the tin-spodumene belt of North Carolina and South Carolina, USA. *Can. Mineral.*, **50**, 1589–1608.

White, J.S. (1981): Mineralogy of the Foote mine, Kings Mountain, North Carolina. *in* ''Geological Investigations of the Kings Mountain belt and adjacent areas in the Carolinas'', Horton J.W. Jr. Butler, J.R. Milton, D.M. eds. Carolina Geological Society, Raleigh, NC, 39.

White, J.S., Arem, J.E., Nelen, J.A., Leavens, P.B., Thomssen, R.W. (1973): Brannockite, a new tin mineral. *Mineral. Rec.*, **3–4**, 73.